Target recognition by calmodulin: the role of acid region contiguous to the calmodulin-binding domain of calcineurin A

Masahiro Noguchi[a], Yoshinobu Izumi[a,*], Hidenori Yoshino[b]

[a]*Graduate Program of Human Sensing and Functional Sensor Engineering, Graduate School of Science and Engineering, Yamagata University, 4-3-16, Jo-nan, Yonezawa 992-8510, Japan*
[b]*Department of Chemistry, Sapporo Medical University, S-l W-17, Chuo-ku, Sapporo 060-0061, Japan*

Received 29 April 2004; revised 13 July 2004; accepted 21 July 2004

Available online 9 August 2004

Edited by Judit Ovádi

Abstract Small-angle X-ray scattering was used to investigate the role of acid region contiguous to the calmodulin-binding domain (391–414) of calcineurin in the target recognition by calmodulin. Three synthetic peptides with the residues 385–414, 380–414 and 374–414 of calcineurin A were used for this aim. The X-ray data are consistent with the fact that calmodulin binds all three peptides with or without Ca^{2+}. Without Ca^{2+}, the whole peptide including acid residues interacts with dumbbell shaped calmodulin, while the acid region is extruded from globular shaped calmodulin with Ca^{2+}. Consequently, a conformation of sequence 374–414 in calcineurin might be changed by Ca^{2+}-signal via calmodulin, suggesting the consequence of this region with acid residues in the full activation mechanism of calcineurin by Ca^{2+}-bound calmodulin.

Keywords: Ca^{2+}-induced extrusion; Calcineurin; Calmodulin; Small-angle X-ray scattering

1. Introduction

Calmodulin (CaM) is a ubiquitous Ca^{2+}-binding protein of 148 residues that regulates a variety of physiological processes in a Ca^{2+}-dependent manner [1]. The regulation is achieved through the interaction of Ca^{2+}-bound CaM (Ca^{2+}/CaM) with a large number of target enzymes [2–4]. The structures of Ca^{2+}/CaM complexed with a CaM-binding domain from target enzymes adopt a compact globular structure caused by the bending of the central linker [5–7]. Recently, however, an extended but not collapsed structure of CaM found in the complexes with a model peptide and the crystal of CaM-regulated adenylate cyclase suggests that CaM should regulate target proteins with versatile ways [8,9]. Moreover, the structure of Ca^{2+}-free CaM (apoCaM) remains unchanged upon binding the CaM-binding domain, except for the decrease of the flexibility of the central linker [10].

The function of calcineurin (Cn) is regulated with Ca^{2+} by dual ways, one is Ca^{2+}-binding to CnB and the other is Ca^{2+}/CaM binding to CnA. A biochemical approach suggested that the Ca^{2+}-binding to CnB caused to release the CaM-binding domain of CnA from its catalytic domain to open the active site partially [11,12]. The following binding of Ca^{2+}/CaM to CnA might open up the active site fully. One of the characteristic features of Ca^{2+}/CaM binding domain of CnA (391–414) [13], which has been classified as 1-5-8-14 motif [14], is that it has a cluster of acidic amino acids at upstream contiguous to the domain. Since there is no evidence for a solution structure of CaM with the CaM-binding domain of CnA so far, we study the structure by small-angle X-ray scattering (SAXS) that is a powerful technique for such measurements. We used three synthetic peptides of residues 385–414, 380–414, and 374–414 of CnA. The present results suggest that the acid region does its share to fully activate Cn by Ca^{2+}-signal via CaM.

2. Materials and methods

2.1. Materials

Table 1 summarizes the primary sequences of three synthetic peptides of CnA (CnAp). These peptides correspond to the residues 385–414, 380–414, and 374–414 of CnA and are denoted hereafter by CnAp385, CnAp380, and CnAp374, respectively. These peptides were synthesized on an Applied Biosystems Model 431A Peptide synthesizer using the general procedure and purified by reverse phase high-performance liquid chromatography [10]. The recombinant CaM based on the sequence of rat CaM was expressed by the method of Hayashi et al. [15]. CaM fraction was obtained according to the trichloroacetic acid (TCA) method of Yazawa et al. [16]. The TCA method provided us Ca^{2+}-free, apoCaM as proved in the previous reports [17,18]. For all experiments, ultrapure water (milli-Q apparatus, Millipore Inc.) and plasticware washed in 1 N HCl were used to minimize calcium contamination.

2.2. SAXS measurements

The basic medium used for the SAXS measurements was 50 mM Tris–HCl, pH 7.6, and 120 mM NaCl. The complexes of apoCaM/CnAp were placed in 1 mM EDTA, while those of Ca^{2+}/CaM/CnAp were prepared by mixing the protein with both a 4.4-fold molar excess of Ca^{2+} and a 1.1-fold molar excess of each peptide. The protein concentrations were 7.5, 10.0, 12.5, 15.0, and 17.5 mg/ml. The concentration of proteins was determined by the method of Lowry et al. [19].

The measurements were performed using synchrotron orbital radiation with an instrument for SAXS installed at BL-10C of Photon Factory, Tsukuba. An X-ray wavelength of 1.488 Å was selected. The temperature of the SAXS experiment was kept at 25.0 ± 0.1 °C by circulating water through the cell holder. The reciprocal parameter, s, equal to $(2\sin\theta)/\lambda$, was calibrated by the observation of a chicken collagen, where 2θ is the scattering angle and λ is the X-ray wavelength. Scattering data were collected for 200 s at various concentrations. The experimental details are described elsewhere [20].

* Corresponding author. Fax: +81-238-26-3177.
E-mail address: yizumi@yz.yamagata-u.ac.jp (Y. Izumi).

0014-5793/$22.00 © 2004 Federation of European Biochemical Societies. Published by Elsevier B.V. All rights reserved.
doi:10.1016/j.febslet.2004.07.079

Table 1
Primary sequences of CnA peptides synthesized in this work

peptide name	primary sequence	AA	*M*
CnAp385	* DGATAAARKEVIRNKIRAIGKMARVFSVLR	30	3298
CnAp380	*** * EEDGFDGATAAARKEVIRNKIRAIGKMARVFSVLR	35	3876
CnAp374	*** *** * DDELGSEEDGFDGATAAARKEVIRNKIRAIGKMARVFSVLR	41	4492

AA represents the number of amino acids.
M represents the molecular weight of CnA peptide.
The putative CaM binding region is underlined.
Acid residue in the acid region of CnA peptide is denoted by an asterisk (*).

Two methods of data analysis were used. The first method was that of Guinier–Fournet [21]. The scattering intensity $I(s,c)$ measured as a function of s at a finite protein concentration, c, is given by:

$$I(s,c) = I(0,c)\exp\{-(4\pi^2/3)R_g(c)^2 s^2\} \quad (1)$$

where $I(0,c)$ is the scattering intensity at $s=0$ and $R_g(c)$ is the radius of gyration at a concentration, c. In the dilute limit, $I(0,c)$ is given by:

$$Kc/I(0,c) = 1/M + 2A_2c + \cdots \quad (2)$$

where K is a constant, M is the molecular weight of the protein, and A_2 is the second virial coefficient. The K value was determined using the Ca^{2+}/CaM sample without peptide as a standard sample. In the dilute limit, R_g is given by:

$$R_g(c)^2 = R_0^2 - B_{if}c + \cdots \quad (3)$$

where R_0 is the radius of gyration at infinite dilution and B_{if} is the parameter of interparticle interference [22]. Using Eqs. (2) and (3), we estimated the four parameters M, A_2, R_0, and B_{if}. For the analysis, the range of s^2 (Å^{-2}) was 2.6×10^{-5}–2.0×10^{-4} for samples in the presence of Ca^{2+}, while it was 2.6×10^{-5}–1.3×10^{-4} in the absence of Ca^{2+}. The second method was the calculation of the distance distribution function, $P(r)$, which provides the structural characteristics such as molecular shape of a protein molecule. $P(r)$ is given by:

$$P(r) = 8\pi\int I(s)(sr)\sin(2\pi sr)\,ds. \quad (4)$$

The maximum length of the complex, d_{max}, was estimated from the $P(r)$ analysis. Other details of data analysis were described elsewhere [23].

The error bars are usually denoted in the case where the experimental errors are larger than the symbols.

3. Results

3.1. Guinier region of the scattering profile in the presence and absence of Ca^{2+}

An example of Guinier plots ($\ln I(s)$ versus s^2) for the CaM/CnAp374 complex in the presence and absence of Ca^{2+} over the concentration series is shown in Fig. 1A and B. In all of the samples studied here, there is no evidence of any upward curvature at low s^2 values in the Guinier plots, which indicates that the data are free from the aggregation of the samples. The values of $Kc/I(0,c)$, evaluated from the intercepts of the Guinier plots for three complexes, are shown in Fig. 2A as a function of protein concentration. The plots are linear over the entire concentration range and the value of $[Kc/I(0,c)]_{c=0}$ extrapolated to infinite dilution for the complex in the presence and absence of Ca^{2+} has the inverse molecular weight appropriate for the soluble monomer. It is noted that the ordinate for the Ca^{2+}/CaM/CnAp385 complex does not extrapolate the same value at zero concentration for apoCaM/CnAp385 complex. Since the ordinate represents the reciprocal of the molecular weight, the corresponding molecular weight is slightly smaller than the calculated value, suggesting that the system is at least free from aggregation. At present, the origin for the smaller value is not clear. The addition of Ca^{2+} to each complex leads to a dramatic reversal of the sign of slopes. The molecular weights M and the second virial coefficients A_2 were calculated using Eq. (2) and compiled in Table 2. The experimental value of M for each complex agrees with the calculated value denoted

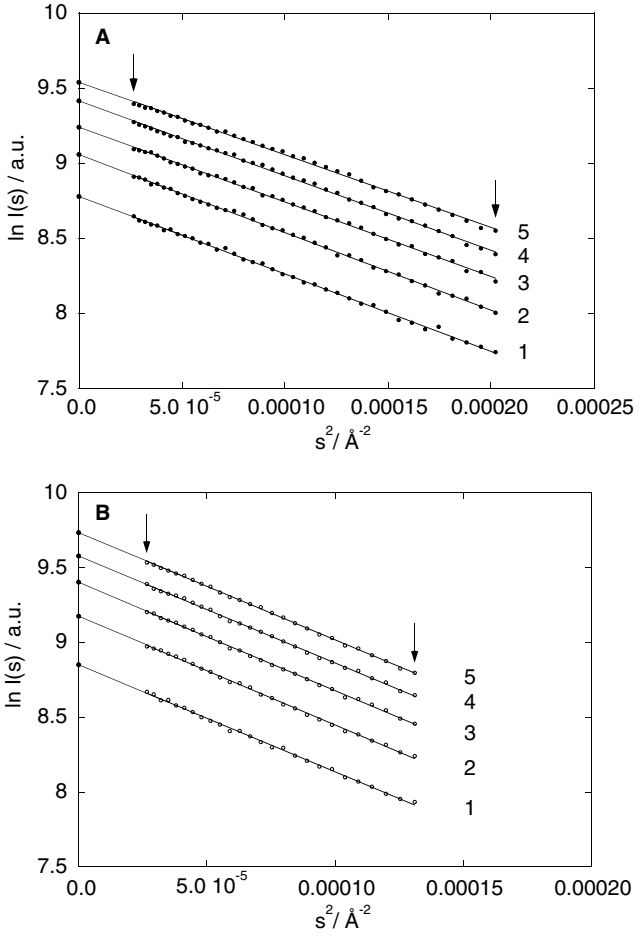

Fig. 1. Guinier plots for Ca^{2+}/CaM/CnAp374-414 (A) and for apoCaM/CnAp374-414 (B) at various protein concentrations: (1) 7.5 mg/ml; (2) 10 mg/ml; (3) 12.5 mg/ml; (4) 15 mg/ml; and (5) 17.5 mg/ml. The straight lines were obtained with the data points between the arrows in the figure by the least square method.

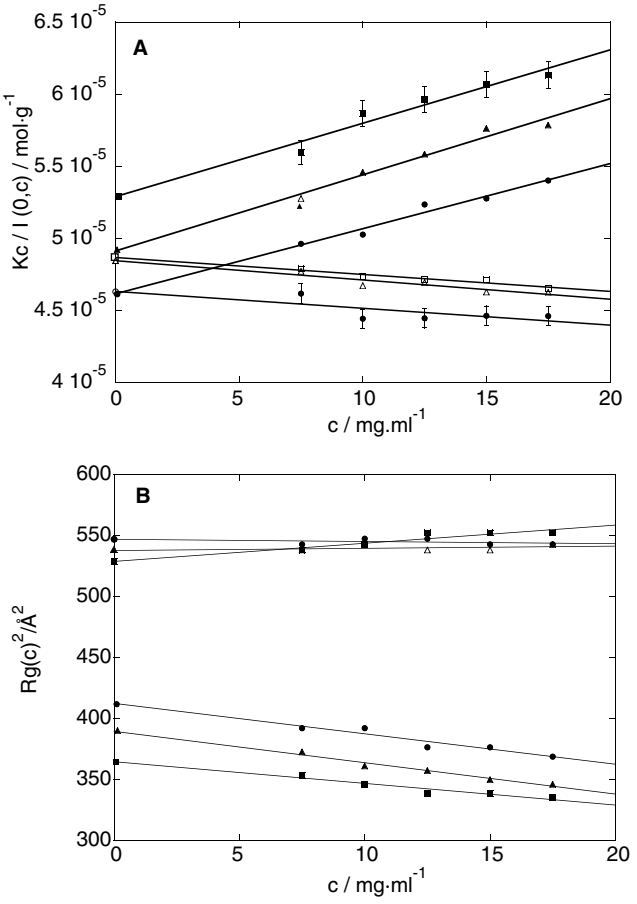

Fig. 2. Zimm plots (A) and the square of radius of gyration, Rg^2, as a function of the protein concentration (B) for complexes of Ca^{2+}/CaM/CnAp and apoCaM/CnAp: Ca^{2+}/CaM/CnAp385 (filled square), Ca^{2+}/CaM/CnAp380 (filled triangle), Ca^{2+}/CaM/CnAp374 (filled circle); apoCaM/CnAp385 (open square), apoCaM/CnAp380 (open triangle), apoCaM/CnAp374 (open circle).

by a parenthesis within the experimental error. Neither of the presence and absence of Ca^{2+} prevents the complex formation. The complex formation is not also prevented by the induction of the acid region. The addition of Ca^{2+} to each complex leads to a dramatic reversal of the sign of A_2.

Radii of gyration at finite concentrations were calculated from the slopes of the Guinier plots using Eq. (1) and are shown in Fig. 2B. The linear increase with decreasing protein concentration was observed in the presence of Ca^{2+}. The slopes of these lines represent a virial coefficient [21]. On the other hand, the slopes in the absence of Ca^{2+} change from positive to small negative value depending on the size of the acid region. Table 2 compiles the values of R_0 and B_{if}.

The R_0 values in the presence of Ca^{2+} are evidently larger than that for the complex of Ca^{2+}/CaM/target peptide with the 1-5-8-14 motif (about 18 Å, which has been reported as a typical value of the compact globular structure [23,24]). The introduction of the acid region enables to increase the R_0 values of the complexes. Besides, the values of R_0 increase with the size of the acid region. The B_{if} value for each complex is positive and the sign remains unchanged by the size of the acid region. On the other hand, the R_0 value for the apoCaM/CnAp complexes is about 23 Å, a typical value of the dumbbell-like structure [10]. The R_0 value remains almost unchanged by the size of the acid region. The B_{if} value for each complex changes from negative to small positive depending on the size of the acid region.

3.2. Result of the $P(r)$ analysis in the presence and absence of Ca^{2+}

Fig. 3 shows scattering profiles normalized by the protein concentration series for the CaM/CnAp complexes in the presence and absence of Ca^{2+}. As shown in panel A of Fig. 3, in the presence of Ca^{2+}, each scattering profile is a monotonous curve which is characteristic of the compact globular structure. As shown in panel B of Fig. 3, in the absence of Ca^{2+}, however, the characteristic feature of each profile has a hump at around $s = 0.03$ Å^{-1} which is characteristic of the dumbbell-like structure. Using each black curve shown in Fig. 3, the distance distribution function $P(r)$ was calculated. Fig. 4A shows a comparison among the $P(r)$ curves for the Ca^{2+}/CaM/CnAp complexes. The maximal $P(r)$ value for the Ca^{2+}/CaM/CnAp385 falls near 24 Å and the d_{max} value is 51 Å, close to a compact globular structure [24]. The values of maximal $P(r)$ and d_{max} are evidently shifted to a larger value of r for the complex with a longer acid region. The difference curves in Fig. 4B represent the $P(r)$ curves with a longer acid region subtracted by the $P(r)$ curve for the Ca^{2+}/CaM/CnAp385 complex. The minimum at around 20 Å decreases, while the maximum at around 45 Å increases, as the acid region lengthens. The increase of the maximum must be

Table 2
M and second virial coefficient (A_2), radius of gyration at infinite dilution (R_0) and parameter of interparticle interference (B_{if}), maximum length evaluated from the $P(r)$ analysis (d_{max}) for CaM/peptide complex in the presence and absence of Ca^{2+} at pH 7.6

Protein	10^{-3} M (calculated value)	$10^4 A_2$ (mol cm^3/g^2)	R_0 (Å)	$10^{13} B_{if}$ (cm^5/g)	d_{max} (Å)
Ca^{2+}/CaM/CnAp385	19.0 ± 1.0 (20.2)	2.5 ± 0.3	19.1 ± 0.3	1.8 ± 0.2	51
Ca^{2+}/CaM/CnAp380	20.3 ± 1.0 (20.7)	2.6 ± 0.3	19.8 ± 0.3	2.6 ± 0.3	53
Ca^{2+}/CaM/CnAp374	21.6 ± 1.1 (21.4)	2.3 ± 0.2	20.3 ± 0.3	2.5 ± 0.3	56
ApoCaM/CnAp385	20.6 ± 1.0 (20.0)	−0.6 ± 0.2	23.0 ± 0.3	−1.5 ± 0.2	66
ApoCaM/CnAp380	20.6 ± 1.0 (20.6)	−0.7 ± 0.2	23.2 ± 0.3	−0.2 ± 0.2	66
ApoCaM/CnAp374	21.6 ± 1.1 (21.2)	−0.6 ± 0.2	23.4 ± 0.3	0.2 ± 0.2	67

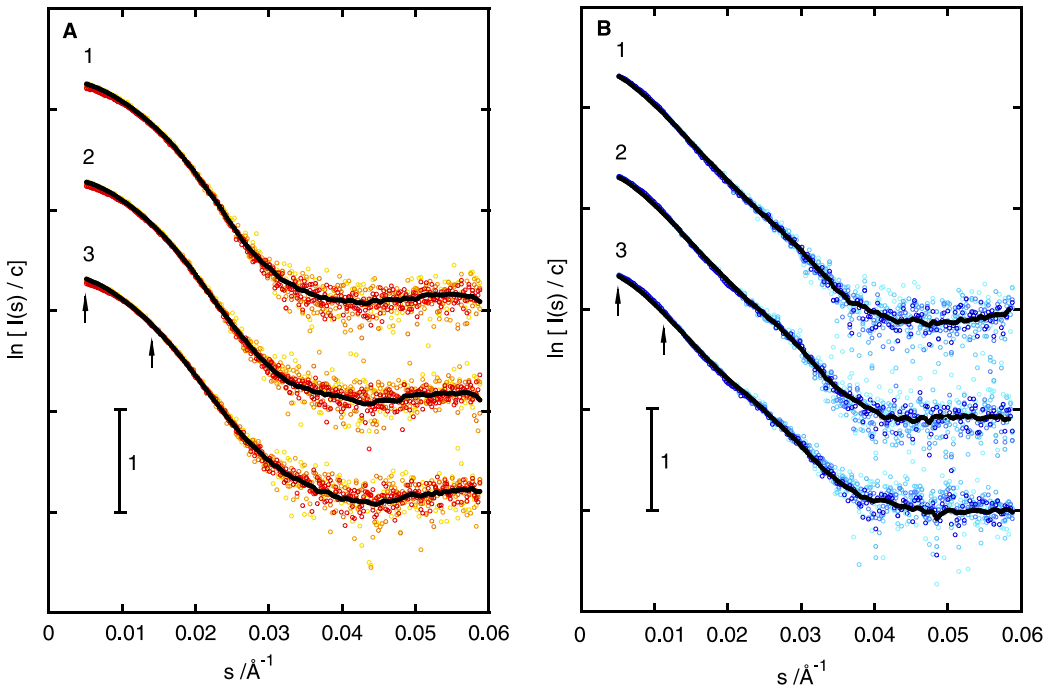

Fig. 3. The SAXS profiles for the CaM/CnAp complexes normalized by the protein concentration series in the presence (A) and absence (B) of Ca^{2+}. The numbers 1 to 3 represent Ca^{2+}/CaM/CnAp385, Ca^{2+}/CaM/CnAp380 and Ca^{2+}/CaM/CnAp374, respectively. Data points between the arrows in the figure were used in the Guinier-Fournet analysis. The ordinate for each complex is shifted as to demonstrate the scattering profile clearly. The scattering profiles for each complex are superimposed over the protein concentration series. The hue shown in the panel A corresponds to that from 7.5 mg/ml (yellow) to 17.5 mg/ml (red), while that in the panel B does that from 7.5 mg/ml (cyan) to 17.5 mg/mol (navy blue). The black curve for each complex is free from the concentration effect and used for the calculation of $P(r)$.

principally connected to an increase in the size of the acid region separated from the compact globular domain.

Fig. 5 shows a comparison among the $P(r)$ curves for apoCaM/CnAp complexes. The $P(r)$ curves remains almost unchanged by the presence of the acid region. That is, the maximal $P(r)$ value falls near 23 Å, the d_{max} value is about 66 Å and a shoulder is observed at around 45 Å, typical of a dumbbell-like structure observed in the complex of apoCaM/CaMKIVp peptide [10].

4. Discussion

The SAXS results presented here show that the R_0 and d_{max} values for the Ca^{2+}/CaM/CnAp complexes increase evidently with the size of the acid region, while those for the apoCaM/CaM/CnAp complexes remain almost unchanged. The most straightforward interpretation of these results is that in the Ca^{2+}-bound conformation, the acid region is extruded to solvent, while in the Ca^{2+}-free conformation, it interacts with a domain in calmodulin.

In developing a molecular explanation for the Ca^{2+}-induced extrusion of the acid region, it is particularly useful to note that even in the presence of any peptide among three, Ca^{2+}/CaM binds to the same CaM-binding domain. As the CnAp peptides with the CaM-binding domain have been classified as the 1-5-8-14 motif, Ca^{2+}/CaM recognizes this motif and adopts a compact globular structure. The R_0 and d_{max} values for the complexes with the acid region are, however, larger than the corresponding values for the compact globular structure. Besides, these values increase evidently with the size of the acid region. The results show that the long axis of the complex crossovers from the axis passing through the two domains of CaM to that of the peptide. If the overall structure of the Ca^{2+}/CaM complexed with the CaM-binding domain of CnA is equivalent to that of the Ca^{2+}/CaM/M13 complex, the long axis of the peptide is about 37 Å [5]. As the acid region of CnAp, in particular, CnAp380 or CnAp374 contains a mass of acid residues, the shape usually adopts an extended conformation. If the extended conformation is described as a worm-like chain [25], the length of the acid region is estimated as 10, 15, and 20 Å for the CnAp385, CnAp380, and CnAp374, respectively. The long axis passing through each peptide is, then, 47, 52, and 57 Å for the Ca^{2+}/CaM/CnAp385, Ca^{2+}/CaM/CnAp380, and Ca^{2+}/CaM/CnAp374 complexes, respectively. These values agree with the experimental values of d_{max} in Table 2. The results provide the evidence that the acid region of the Ca^{2+}/CaM/CnAp complex is extruded to solvent in the Ca^{2+}-bound conformation.

The difference curves in Fig. 4B represent that the minimum at around 20 Å decreases with the size of the acid region, while the maximum at around 45 Å increases. As the maximum must relate principally to the distance between the compact globular domain and the acid region, the increase of the maximum is connected to the increase of the size of the acid region. The driving force for the extrusion of the acid region may be principally derived from the electrostatic repulsion between Ca^{2+}/CaM and the acid region of the peptide, which corresponds to large positive values of A_2 and B_{if}.

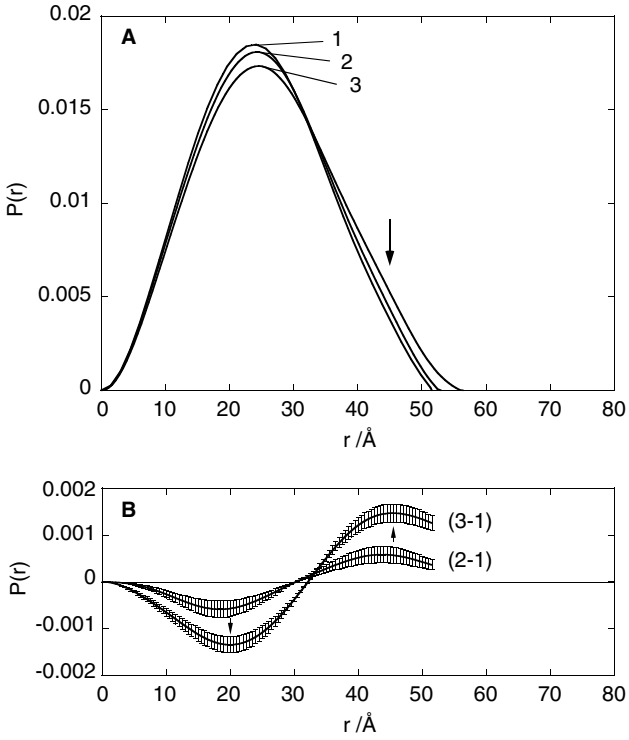

Fig. 4. Distance distribution functions, $P(r)$, (A) and the difference curves, ΔP(r), (B) for Ca^{2+}/CaM/CnAp complexes. The numbers 1 to 3 represent Ca^{2+}/CaM/CnAp385, Ca^{2+}/CaM/CnAp380 and Ca^{2+}/CaM/CnAp374, respectively. The arrow at around 45 Å relates principally to distances between the compact globular structure in the complex and the acid region in the peptide. The decrease at around 20 Å in the $P(r)$ curve is linked with the increase at around 45 Å, as the integrated value of $P(r)$ curve is normalized.

The apoCaM/CnAp complex adopts a dumbbell-like structure utilizing a binding motif as observed in the apoCaM/CaMKIVp [10]. The R_0 and d_{max} values for the complexes remain almost unchanged by the size of acid region. Residues 380–384 of CnAp380 and 374–384 of CnAp374 do not cause any increase in these values, suggesting that these residues

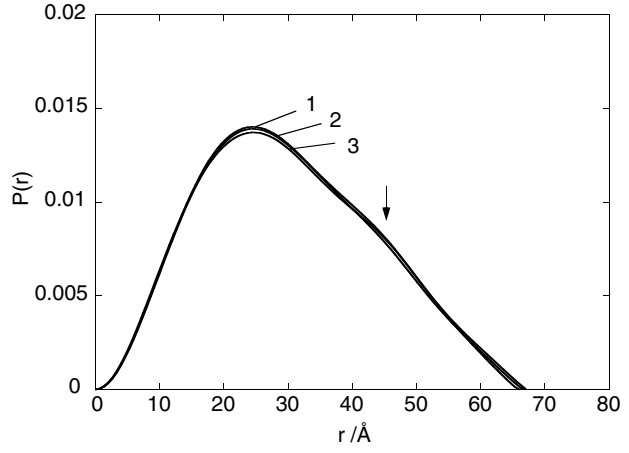

Fig. 5. Distance distribution functions, $P(r)$, for apoCaM/CnAp complexes. The numbers 1 to 3 represent apoCaM/CnAp385, apoCaM/CnAp380 and apoCaM/CnAp374, respectively. The arrow at around 45 Å represents a shoulder characteristic of the dumbbell-like structure.

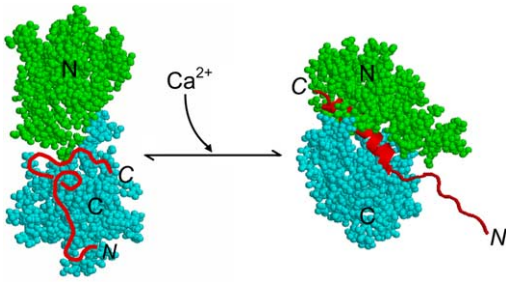

Fig. 6. Schematic model of Ca^{2+}-indueed extrusion of the acid region of calcineurin. In the Ca^{2+}-free conformation (Left), both the acid region and CaM-binding domain in calcineurin A directly interact with a domain of CaM, which adopts a dumbbell-like structure. In the Ca^{2+}-bound conformation (Right), CaM complexed with the CaM-binding domain adopts a compact globular structure, while the acid region is extruded from the compact structure to solvent. The symbols N and C denote the N-and C-termini of CaM or CnAp, respectively. The protein data bank code for the structures are 3CLN and 2BBM for apoCaM alone and Ca^{2+}/CaM/CnAp complex, respectively.

interact directly with a domain of calmodulin. The shapes of the $P(r)$ curves for these complexes shown in Fig. 5 are almost superimposed with each other regardless of the difference of acid residues, suggesting again that the whole peptides including acid residues bind to a domain of apoCaM.

Fig. 6 presents a model to account for the SAXS results. In the Ca^{2+}-free conformation (Left), almost disordered peptide including both the acid region and CaM-binding domain directly interacts with a domain of CaM, which adopts a dumbbell-like structure. On the other hand, in the Ca^{2+}-bound conformation (Right), the CaM complexed with the CaM-binding domain adopts a compact globular structure and the acid region is extruded to solvent. Thus, Ca^{2+} signals induce a conformational change of the peptides via CaM.

The region of 374–414 of CnA, which is located just downstream of the binding site for CnB, might be a disordered structure, because this region was invisible in the crystal without CaM [26]. The crystal structure of calcineurin in the presence of CaM has not been presented until now. Therefore, a similar conformational change of 374–414 region shown in Fig. 6 likely occurs even in CnA by Ca^{2+} signals via CaM irrespective of the binding of apoCaM to CnA. The conformational change described may cause to move the large segment of residues from 374 to C-terminal end, allowing the full active structure for Cn. Here, it should be emphasized that not only the CaM binding domain in Cn (391–414) but also the acid residues are functioning to fully activate Cn with Ca^{2+} signals synergetically.

The R_g values of CaM with a model peptide corresponding to the CaM binding domain in Cn decreased with an increasing Ca^{2+} concentration up to 4-mol of Ca^{2+}/mol of CaM (data not shown). The result is very similar to the Ca^{2+}-dependent change of R_g obtained with mastoparan, which has the same CaM binding motif as Cn [27]. Therefore, it should be reasonable that the structure shown at right side in Fig. 6 is complete when four Ca^{2+}-binding sites of CaM had been occupied. These considerations are consistent with early report presented by Kincaid and Vaughan [28].

Since we have no evidence for the binding affinities of these peptides to apoCaM so far, it is difficult to refer whether Cn binds apoCaM or not in living cells. Recently, Mori et al. showed a possible enrichment of local CaM in living cells [29].

Acknowledgements: We thank Dr. Katsumi Kobayashi for his help in the SR-SAXS measurements and Dr. Nobuhiro Hayashi for providing plasmids for expression of CaM in *E. coli*. The SAXS measurements were performed with the approval of the Photon Factory Committee, KEK, Tsukuba, Japan (Proposal Nos. 97G130, 99G350 and 01G365).

References

[1] Eldik, L.J.V. and Watterson, D.M. (1998) Calmodulin and Calcium Signal Transduction. Academic Press, San Diego.
[2] Means, A.R., VanBerkum, M.F.A., Bagchi, I., Lu, K.P. and Rasmussen, C.D. (1991) Pharmacol. Ther. 50, 255–270.
[3] Vogel, H.J. (1994) Biochem. Cell. Biol. 72, 357–376.
[4] James, P., Vorherr, T. and Carafoli, E. (1995) Trends Biochem. Sci. 20, 38–42.
[5] Ikura, M., Clore, G.M., Gronenborn, A.M., Zhu, G., Klee, C.B. and Bax, A. (1992) Science 256, 632–638.
[6] Meador, W.E., Means, A.R. and Quiocho, F.A. (1992) Science 257, 1251–1255.
[7] Meador, W.E., Means, A.R. and Quiocho, F.A. (1993) Science 262, 1718–1721.
[8] Hoeflich, K.P. and Ikura, M. (2002) Cell 108, 739–742.
[9] Ikura, M., Osawa, M. and Ames, J.B. (2002) BioEssays 24, 625–636.
[10] Izumi, Y., Kuwamoto, S., Jinbo, Y. and Yoshino, H. (2001) FEBS Lett. 495, 126–130.
[11] Stemmer, P.M. and Klee, C.B. (1994) Biochemistry 33, 6859–6866.
[12] Yang, S.-A. and Klee, C.B. (2000) Biochemistry 39, 16147–16154.
[13] Ito, A., Hashimoto, T., Hirai, M., Takeda, T., Shuntoh, H., Kuo, T. and Tanaka, G. (1989) Biochem. Biophys. Res. Commun. 163, 1492–1497.
[14] Rhoads, A.R. and Friedberg, F. (1997) FASEB J. 11, 331–340.
[15] Hayashi, N., Matsubara, M., Takasaki, A., Titani, K. and Taniguchi, H. (1998) Protein Expr. Purif. 12, 25–28.
[16] Yazawa, M., Sakuma, M. and Yagi, K. (1980) J. Biochem. 87, 1313–1320.
[17] Minowa, O. and Yagi, K. (1984) J. Biochem. 96, 1175–1182.
[18] Nakashima, K., Maekawa, H. and Yazawa, M. (1996) Biochemistry 35, 5602–5610.
[19] Lowry, O.H., Rosebrough, N.J., Farr, A.L. and Randall, R.J. (1951) J. Biol. Chem. 193, 265–275.
[20] Ueki, T., Hiragi, Y., Kataoka, M., Inoko, Y., Amemiya, Y., Izumi, Y., Tagawa, H. and Muroga, Y. (1985) Biophys. Chem. 23, 115–124.
[21] Guinier, A. and Fournet, G. (1955) Small-Angle Scattering of X-rays. Wiley, New York. pp. 24–28, 40–52, 57–60, 126–136.
[22] Izumi, Y., Wakita, M., Yoshino, H. and Matsushima, N. (1992) Biochemistry 31, 12266–12271.
[23] Matsushima, N., Izumi, Y., Matsuo, T., Yoshino, H., Ueki, T. and Miyake, Y. (1989) J. Biochem. 105, 883–887.
[24] Yoshino, H., Izumi, Y., Sakai, K., Takezawa, H., Matsuura, I., Maekawa, H. and Yazawa, M. (1996) Biochemistry 35, 2388–2393.
[25] Konishi, T., Toshizaki, T., Saito, T., Einaga, Y. and Yamakawa, H. (1990) Macromolecules 23, 290–297.
[26] Kissinger, C.R., Parge, H.E., Knighton, D.R., Lewis, C.T., Pelletier, L.A., Tempczyk, A., Kalish, V.J., Tucker, K.D., Showalter, R.E., Moomaw, E.W., Gastinel, L.N., Habuka, N., Chen, X., Maldonado, F., Barker, J.E., Bacquet, R. and Villafranca, J.E. (1995) Nature 378, 641–644.
[27] Yoshino, H., Minari, O., Matsushima, N., Ueki, T., Miyake, Y., Matsuo, T. and Izumi, Y. (1989) J. Biol. Chem. 264, 19706–19709.
[28] Kincaid, R.L. and Vaughan, M. (1986) Proc. Natl. Acad. Sci. USA 83, 1193–1197.
[29] Mori, M.X., Erickson, M.G. and Yue, D.T. (2004) Science 304, 432–435.